

Determination of cross sections for collisionally induced multipole relaxation in alkali-metal atoms from Zeeman fluorescence intensities

R. W. Berends, W. Kedzierski, W. E. Baylis, and L. Krause
 Department of Physics, University of Windsor, Windsor, Ontario, Canada N9B 3P4
 (Received 20 June 1988)

The determination of cross sections for the relaxation of atomic multipole moments from the intensities of the components of a resolved Zeeman fluorescence spectrum may be carried out using the density-matrix formalism. However, the spherical-tensor basis is not well adapted to state-selected measurements and can allow a significant propagation of error. We can reduce the error by determining the $Q(j, m \rightarrow j', m')$ cross sections directly from the data taken at the lowest pressures. A comparison is given between recent experimental and theoretical relaxation cross sections for collisions of 5^2P potassium atoms with ground-state He, Ne, and Ar atoms.

We have recently reported the results of an experiment in which we determined the cross sections for relaxation of the atomic dipole, quadrupole, and octupole moments in 5^2P potassium atoms by collisions with ground state He, Ne, and Ar atoms, as well as the cross sections for collisional mixing between the 5^2P Zeeman substates.^{1,2} In comparing the experimental values of the relaxation cross sections with theoretical calculations of Spielfiedel *et al.*³ we became aware of very large discrepancies between the two sets of values. Most recently, two additional calculations came to our attention. Pascale⁴ calculated the multipole relaxation and Zeeman-mixing cross sections for collisions with He atoms, and Spielfiedel and Feautrier⁵ carried out the corresponding calculation for Ne collisions, both with improved interatomic potentials. It appeared that some of the most recently calculated Zeeman-mixing cross sections agreed very well with the experimental values but others did not, as may be seen in Table I. As a result, there were still substantial differences between the calculated and measured relaxation cross sections. In our attempts to reconcile the theoretical and experimental results, particularly for the relaxation cross sections, we became aware of some problems connected with the determination of the relaxation cross sections from the experimental data, which arise from excessive propagation of error. A re-analysis of the relaxation cross sections has been carried out by using the available experimental data at low pressure, resulting in a substantial reduction in the propagated error and yielding values of the relaxation cross sections in much better agreement with the more recent theoretical values.

The description of the experiment and the representation of the system using the density-matrix formalism, may be found elsewhere.¹ When only diagonal elements of the density matrix are excited and the collisions are isotropic, off-diagonal elements vanish.⁶ The rate equations which take account of the processes of excitation, spontaneous decay, and collisional Zeeman and fine-structure (FS) mixing, have approximate solutions for the multipole relaxation cross sections Λ in terms of the time-integrated intensities of the Zeeman fluorescence components, stated by Eqs. (19) and (20) in Ref. 1. These equations neglect second-order and higher products of FS transfers and assume that the collisional quenching of the

5^2P state is negligible. In order to determine the multipole-relaxation cross sections with these solutions, it is necessary to know the depopulation cross sections $\sigma_{ii}^{(0)}$. Furthermore, the factors $[K_{ii}^{0L} - 1]$ appearing in the solutions, tend to magnify the errors in the populations $n^{(L)}$ as measured in our experiment.² We have found alternative solutions of the rate equations which avoid the approximations and assumptions implicit in Eqs. (19) and (20) of Ref. 1,

$$N v_r \tau_i \left[K_{ii}^{01} \frac{(1 - K^{(0)})}{1 - K^{(1)}} - 1 \right]^{-1} = \frac{1}{\Lambda_{ii}^{(1)}} + N v_r \tau_i \frac{\sigma_{ii}^{(0)}}{\Lambda_{ii}^{(1)}}, \quad i = 1, 2 \quad (1)$$

$$N v_r \tau_2 [K_{22}^{0L} (1 - K^{(0)}) - 1]^{-1} = \frac{1}{\Lambda_{22}^{(L)}} + N v_r \tau_2 \frac{\sigma_{22}^{(0)}}{\Lambda_{22}^{(L)}}, \quad L = 2, 3 \quad (2)$$

where

$$K^{(L)} = \begin{pmatrix} n_2^{(L)} \\ n_1^{(L)} \end{pmatrix}_1 \begin{pmatrix} n_1^{(L)} \\ n_2^{(L)} \end{pmatrix}_2, \quad L = 0, 1 \quad (3)$$

is the product of the $(2L + 1)$ -pole ratios of the collisionally populated FS state to the directly populated FS state (the subscript on the parenthesis indicates which FS state was directly excited). The notation is identical to that used in Ref. 1.

Equations (1) and (2) are in the form $Y = A + BX$, where X is proportional to the pressure; A , the low-pressure intercept of Y , is the inverse of the relaxation cross section Λ , and the slope B corresponds to the ratio of the depopulation cross section $\sigma^{(0)}$ to the relaxation cross section and is a measure of the rate at which the multipole-population-density distributions reach equilibrium. Although Eqs. (1) and (2) are improvements over Eqs. (19) and (20) of Ref. 1 and may prove useful when analyzing polarized fluorescence from systems excited at low magnetic fields with polarized radiation, they suffer from the same error-propagation problems when used with state-selected excitation and detection. The relaxation cross sections are related to the Zeeman-mixing cross section $Q(j, m \rightarrow j', m')$ by^{3,6}

$$\Lambda_{1/2}^{(1)} = 2Q(\frac{1}{2} - \frac{1}{2} \rightarrow \frac{1}{2} \frac{1}{2}), \quad (4)$$

TABLE I. 5P Zeeman-mixing cross sections for collisions with He, Ne, and Ar. $Q(J, M \rightarrow J', M')$ (10^{-16} cm²).

Designation	Ref.	Collision partner			Designation	Ref.	Collision partner		
		He	Ne	Ar			He	Ne	Ar
$Q(\frac{1}{2}, -\frac{1}{2} \rightarrow \frac{1}{2}, +\frac{1}{2})$	2	95±7	73±9	80±11	$Q(\frac{3}{2}, -\frac{3}{2} \rightarrow \frac{3}{2}, +\frac{1}{2})$	2	80±15	81±3	70±5
	4	74				4	108		
	5		63			5		101	
$Q(\frac{1}{2}, -\frac{1}{2} \rightarrow \frac{3}{2}, +\frac{3}{2})$	2	78±6	35±5	54±2	$Q(\frac{3}{2}, -\frac{3}{2} \rightarrow \frac{3}{2}, -\frac{1}{2})$	2	137±26	125±11	142±29
	4	79				4	127		
	5		17			5		121	
$Q(\frac{1}{2}, -\frac{1}{2} \rightarrow \frac{3}{2}, +\frac{1}{2})$	2	77±7	36±4	47±6	$Q(\frac{3}{2}, -\frac{3}{2} \rightarrow \frac{1}{2}, +\frac{1}{2})$	2	102±17	74±3	110±26
	4	68				4	85		
	5		15			5		19	
$Q(\frac{1}{2}, -\frac{1}{2} \rightarrow \frac{3}{2}, -\frac{1}{2})$	2	139±4	73±8	94±8	$Q(\frac{3}{2}, -\frac{3}{2} \rightarrow \frac{1}{2}, -\frac{1}{2})$	2	62±9	50±4	57±7
	4	56				4	48		
	5		14			5		13	
$Q(\frac{1}{2}, -\frac{1}{2} \rightarrow \frac{3}{2}, -\frac{3}{2})$	2	94±7	61±3	68±5	$Q(\frac{3}{2}, -\frac{1}{2} \rightarrow \frac{3}{2}, +\frac{1}{2})$	2	135±34	121±15	157±35
	4	45				4	73		
	5		12			5		79	
$Q(\frac{3}{2}, -\frac{3}{2} \rightarrow \frac{3}{2}, +\frac{3}{2})$	2	59±10	61±3	61±5	$Q(\frac{1}{2}, -\frac{1}{2} \rightarrow \frac{3}{2}, -\frac{3}{2})$ $Q(\frac{3}{2}, -\frac{3}{2} \rightarrow \frac{1}{2}, -\frac{1}{2})$	2	1.5	1.2	1.2
	4	48				4	0.94		
	5		52			5		0.92	
					a	0.95	0.95	0.95	

^aPredicted by detailed balance.

$$\Lambda_{3/2}^{(1)} = 2Q(\frac{3}{2} - \frac{3}{2} \rightarrow \frac{3}{2} \frac{3}{2}) + \frac{4}{3}Q(\frac{3}{2} - \frac{3}{2} \rightarrow \frac{3}{2} \frac{1}{2}) + \frac{2}{3}Q(\frac{3}{2} - \frac{3}{2} \rightarrow \frac{3}{2} - \frac{1}{2}), \quad (5)$$

$$\Lambda_{3/2}^{(2)} = 2Q(\frac{3}{2} - \frac{3}{2} \rightarrow \frac{3}{2} \frac{1}{2}) + 2Q(\frac{3}{2} - \frac{3}{2} \rightarrow \frac{3}{2} - \frac{1}{2}), \quad (6)$$

$$\Lambda_{3/2}^{(3)} = 2Q(\frac{3}{2} - \frac{3}{2} \rightarrow \frac{3}{2} \frac{3}{2}) - 2Q(\frac{3}{2} - \frac{3}{2} \rightarrow \frac{3}{2} \frac{1}{2}) + 4Q(\frac{3}{2} - \frac{3}{2} \rightarrow \frac{3}{2} - \frac{1}{2}). \quad (7)$$

The fine-structure-mixing cross sections and orientation-transfer cross sections are similarly defined by Eqs. (4)–(7) in Ref. 1.

In order to reduce the error propagation in the analysis, it was found best to determine the individual Zeeman-mixing cross section $Q(j, m \rightarrow j', m')$ from the slopes of plots of the experimental fluorescence intensity ratios (of the collisionally to directly populated Zeeman sublevels) in relation to $Nv\tau$, which have been shown previously¹ plotted in relation to the buffer-gas pressures. In general, these experimental plots exhibit a nonlinearity with buffer-gas pressures when the pressure is sufficiently high that multiple collisional transfers take place between the Zeeman sublevels. The slopes of these plots are proportional to the corresponding Zeeman-mixing cross sections under single-collision conditions, where $NvQ(J, m \rightarrow J', m')\tau \ll 1$. In our experiment¹ the data were obtained under virtually single-collision conditions, with $NvQ(J, m \rightarrow J', m')\tau \leq 0.3$. In order to verify that the slopes of the plots under these conditions are an accurate measure of the Zeeman-mixing cross sections, we performed a computer simulation of the population density of the Zeeman sublevels, in relation to the buffer-gas

pressures, using the measured Zeeman-mixing cross sections; a sample of the results for K $5^2P_{3/2}$ atoms in collisions with He is shown in Fig. 1. The simulation agrees with the experimentally observed trends and indicates that the expected curvature due to multiple collisions is sufficiently small that the error associated with the linear low-pressure approximation falls within the limits stated in Table I, which represent the statistical scatter of the data. The multipole-relaxation cross sections may be calculated from the individual Zeeman-mixing cross sections using Eqs. (4)–(7). The low-pressure restriction has the advantage of a significant decrease in the propagation of experimental error, the simplicity of the j, m -state basis set for the computer simulation instead of the spherical basis set which defines the Zeeman-multipole densities, and does not require the *a priori* knowledge of the FS-transfer and -depopulation cross sections which introduce additional experimental error.

The experimental values presented in Table I and the theoretical values of Pascale⁴ correspond to the thermally averaged cross sections obtained at 388 K. The theoretical cross sections of Spielfiedel *et al.*³ and Spielfiedel and Feautrier⁵ were calculated for relative velocities corresponding to 450 and 508 K, respectively. The experimental and theoretical Zeeman-mixing cross sections for He agree quite well, except for $Q(\frac{1}{2}, -\frac{1}{2} \rightarrow \frac{3}{2}, -\frac{1}{2})$ and $Q(\frac{1}{2}, -\frac{1}{2} \rightarrow \frac{3}{2}, -\frac{3}{2})$. These cross sections were obtained from clearly resolved spectral components obtained simultaneously with the data from which the other mixing cross sections were obtained, and were consistent in all experimental runs as indicated by the standard devia-

tions. With Ne as collision partner, the experimental and calculated cross sections agree well for Zeeman mixing within the excited FS state, but not nearly as well for mixing between Zeeman sublevels belonging to different FS states. The Zeeman-mixing cross sections $Q(\frac{1}{2}, -\frac{1}{2} \rightarrow \frac{3}{2}, -\frac{3}{2})$ and $Q(\frac{3}{2}, -\frac{3}{2} \rightarrow \frac{1}{2}, -\frac{1}{2})$ were determined individually and their ratio is shown in Table I together with the ratios of the corresponding calculated values and the ratio predicted by the principle of detailed balancing.⁷

The FS and orientation-transfer cross sections $\sigma^{(0)}$ and $\sigma^{(1)}$, respectively, which were derived from the Zeeman-mixing cross sections, are listed in Table II together with the theoretical values calculated by Spielfiedel *et al.*,³ Pascale,⁴ and Spielfiedel and Feautrier.⁵ The error limits accompanying the experimental cross sections were derived from the weighted sums of the standard deviations of the individual Zeeman-mixing cross sections from which the transfer and relaxation cross sections were calculated. The FS-transfer cross sections provided a useful check against the values determined in zero field,⁸ which are also listed in Table II. There is agreement (within error) between the experimental cross sections obtained at 70 kG and those determined in zero field for Ne and Ar, though the agreement for He is not as good. The difference between the calculated cross sections and experimental high-field data, particularly for the case of Pascale's⁴ calculation, arises from a disagreement between the calculated and measured cross sections $Q(\frac{1}{2}, -\frac{1}{2} \rightarrow \frac{3}{2}, -\frac{3}{2})$ and $Q(\frac{1}{2}, -\frac{1}{2} \rightarrow \frac{3}{2}, -\frac{3}{2})$.

The comparison of the orientation-transfer cross sec-

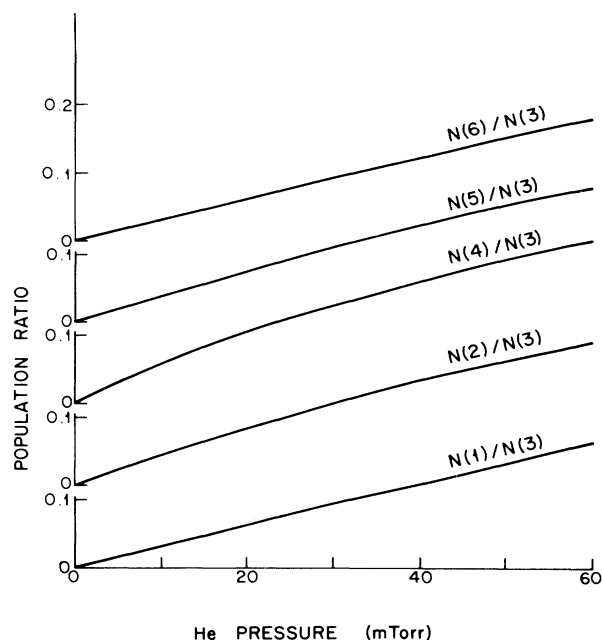


FIG. 1. Plots of the Zeeman-population ratios obtained from a computer simulation of the relaxation of the 5P Zeeman manifold, showing the effects of mixing induced in K-He collisions. The $5^2P_{3/2, -3/2}$ Zeeman substate was optically excited. The population densities of the Zeeman substates are labeled as follows: $N(1) = (\frac{1}{2}, -\frac{1}{2})$; $N(2) = (\frac{1}{2}, +\frac{1}{2})$; $N(3) = (\frac{3}{2}, -\frac{3}{2})$; $N(4) = (\frac{3}{2}, -\frac{1}{2})$; $N(5) = (\frac{3}{2}, +\frac{1}{2})$; $N(6) = N(\frac{3}{2}, +\frac{3}{2})$.

TABLE II. 5P fine-structure-mixing and orientation-transfer cross sections (10^{-16} cm^2).

Designation	Reference	Collision partner		
		He	Ne	Ar
$\sigma_{12}^{(0)}(\frac{1}{2} \rightarrow \frac{3}{2})$	2	274±17	145±14	186±15
	8	397±59	139±20	224±32
	3	156	77	139
	4	174		
	5		41	
$\sigma_{21}^{(0)}(\frac{3}{2} \rightarrow \frac{1}{2})$	2	232±37	175±10	236±47
	8	376±55	139±25	216±31
	4	187		
	5		45	
$\frac{\sigma_{12}^{(0)}(\frac{1}{2} \rightarrow \frac{3}{2})}{\sigma_{21}^{(0)}(\frac{3}{2} \rightarrow \frac{1}{2})}$	2	1.18	0.82	0.79
	8	1.05	1	1.03
	4	0.93		
	5		0.91	
	a	0.93	0.93	0.93
$\sigma_{12}^{(1)}(\frac{1}{2} \rightarrow \frac{3}{2})$	2	35±16	36±11	28±11
	3	-66	-22	-52
	4	-36		
	5		-5	
$\sigma_{21}^{(1)}(\frac{3}{2} \rightarrow \frac{1}{2})$	2	-41±27	-26±7	-56±35
	4	-39		
	5		-6	

^aPredicted by detailed balance.

TABLE III. $5P$ multipole-relaxation cross sections (10^{-16} cm 2).

Designation	Reference	Collision partner		
		He	Ne	Ar
$\Lambda_{1/2}^{(1)}$	2	190±14	145±18	160±22
	3	40.5	258	109
	4	149		
	5		125	
$\Lambda_{3/2}^{(1)}$	2	316±57	314±17	312±36
	3	155	340	253
	4	325		
	5		321	
$\Lambda_{3/2}^{(2)}$	2	434±82	411±28	425±68
	3	256	725	504
	4	471		
	5		445	
$\Lambda_{3/2}^{(3)}$	2	506±154	462±56	551±136
	3	236		438
	4	388		
	5		387	

tions with the calculations of Spielfiedel³ and Pascale⁴ is interesting in that, although the magnitudes of the cross sections are similar, the transfer direction for $\sigma^{(1)}(\frac{1}{2} \rightarrow \frac{3}{2})$ is different. This difference in sign is consistent for all the buffer gases as indicated in Table II. It may be seen in Table I that, in each case, the cross sections $Q(\frac{1}{2}, -\frac{1}{2} \rightarrow \frac{3}{2}, -\frac{3}{2})$ and $Q(\frac{1}{2}, -\frac{1}{2} \rightarrow \frac{3}{2}, -\frac{1}{2})$ are larger than $Q(\frac{1}{2}, -\frac{1}{2} \rightarrow \frac{3}{2}, +\frac{3}{2})$ and $Q(\frac{1}{2}, -\frac{1}{2} \rightarrow \frac{3}{2}, +\frac{1}{2})$, respectively, indicating the preferred excitation transfer to the negative m_j components of the collisionally populated FS Zeeman manifold, contrary to the theoretical predictions. This is equivalent to the preservation of orientation during the collisional interaction, which was not observed with the Na(3P) atoms.⁹ However, the orientation transfer cross section $\sigma^{(1)}(\frac{3}{2} \rightarrow \frac{1}{2})$ for He agrees both in magnitude and direction with the predicted value. The disagreement in the sign of the orientation transfer direction for the transition $5^2P_{1/2} \rightarrow 5^2P_{3/2}$ may be due to the large Zeeman splitting. The energy difference between the $5^2P_{1/2, -1/2}$ and the $5^2P_{3/2, -3/2}$ states is 13.3 cm $^{-1}$ while the energy difference between the $5^2P_{1/2, -1/2}$ and the $5^2P_{3/2, +3/2}$ states is 26.4 cm $^{-1}$. Although the Boltzmann factor is not appreciably different for these two cases, nevertheless the difference in energy splitting is non-negligible compared to the inverse collision time, which would suggest a greater probability of excitation transfer between states with relatively smaller energy separation. This conclusion is verified by the Zeeman-mixing cross sections shown in Table I. Although the slower collisions of the heavier noble-gas partners might

be expected to show a larger difference in the cross sections than He, the interactions are also stronger with the more polarizable Ne and, especially, Ar.

The multipole-relaxation cross sections for collisions with He, Ne, and Ar are presented in Table III. They were calculated from the Zeeman-mixing cross sections listed in Table I using Eqs. (4)–(7). Table III also includes three sets of theoretical cross sections. Some of the earlier values of Spielfiedel *et al.*³ are in good agreement with the experimental results, and some clearly disagree. The more recent Ne calculations⁵ are in much better agreement with the measured cross sections, as are those of Pascale for He.⁴

All the theoretical calculations indicate that, for $P_{3/2}$ relaxation, the cross section for quadrupole relaxation should be the largest. This trend, though noted for Na(3P) in collisions with noble gases by Gay and Schneider⁹ and for K(4P) by Skalinski and Krause¹⁰ and Boggy and Franz,¹¹ is not clearly borne out in the present experiment in which the octupole-relaxation cross section is consistently the largest. The large uncertainty present in the octupole relaxation cross sections may mask the theoretically predicted trend, but it is also possible that the relatively large Zeeman splitting between the $5^2P_{3/2-3/2}$ and the $5^2P_{3/2+3/2}$ (13-cm $^{-1}$) states, due to the strong magnetic field, may have enhanced the measured octupole-relaxation cross section.

This research was supported by a grant from the Natural Sciences and Engineering Research Council of Canada.

¹R. W. Berends, W. Kedzierski, and L. Krause, *Phys. Rev. A* **37**, 68 (1988).

²R. W. Berends, Ph.D. thesis, University of Windsor, 1988.

³A. Spielfiedel, D. Gilbert, E. Roueff, and F. Rostas, *Phys. B* **12**, 3693 (1979).

⁴J. Pascale (private communication).

⁵A. Spielfiedel and N. Feautrier (private communication).

⁶W. E. Baylis, in *Progress in Atomic Spectroscopy*, edited by W. Hanle and H. Kleinpoppen (Plenum, New York, 1979), Part

B, p. 1227.

⁷J. Ciurylo and L. Krause, *J. Quant. Spectrosc. Radiat. Transfer* **28**, 457 (1982).

⁸R. W. Berends, W. Kedzierski, and L. Krause, *J. Quant. Spectrosc. Radiat. Transfer* **37**, 157 (1987).

⁹J.-C. Gay and W. B. Schneider, *Z. Phys. A* **278**, 211 (1976).

¹⁰P. Skalinski and L. Krause, *Phys. Rev. A* **26**, 3338 (1982).

¹¹R. Boggy and F. A. Franz, *Phys. A* **25**, 1887 (1982).